Fizika Nizkikh Temperatur, 1997, v. 23, Nos. 5/6, p. 537–545

# Viscosity and ultrasonic attenuation in $^4$He below 0.6 K

Chung-In Um

*Department of Physics, College of Science, Korea University, Seoul 136-701, Korea*

Soo-Young Lee

*The Research Institute of Basic Science, Korea University, Seoul 136-701, Korea*

Sahng-Kyoon Yoo

*Department of Physics, Seonam University, Namwon, Chunbuk 590-170, Korea*

T. F. George

*Office of the Chancellor / Departments of Chemistry and Physics and Astronomy, University of Wisconsin-Stevens Point, Stevens Point, Wisconsin 54481-3897, U.S.A.*
E-mail: tgeorge@uwsp.edu

L. N. Pandey

*Departments of Chemistry and Physics, Washington State University, Pullman, Washington 99164-4630, U.S.A.*

I. N. Adamenko

*Department of Physics and Technology, Kharkov State University, Kharkov 310077, Ukraine*

Submitted November 29, 1996

Through a treatment of three-phonon processes, the wide-angle scattering rates and the absorption rates of phonons, which characterize viscosity and ultrasonic attenuation, respectively, are calculated for $^4$He below 0.6 K. These rates are obtained from the collision matrix which is constructed approximately from an integral eigenvalue equation for the collision operator. The sequence of the lowest eigenvalues of the collision matrix, as the angular momentum quantum number $l$ increases, shows a saturated behavior which has not been reported before. The calculated viscosity and ultrasonic attenuation are compared with previous theoretical and experimental results.

PACS: 67.40.Pm

## 1. Introduction

Since the anomalous phonon energy spectrum for $^4$He was proposed [1], its transport properties have been studied based on that spectrum [2–4]. For the case of the anomalous phonon spectrum, the lowest-order phonon processes are three-phonon processes (3PP), while for the case of the normal spectrum they are four-phonon processes (4PP). Thus, in order to investigate the properties of superfluid $^4$He at low temperatures, we have to completely understand 3PP.

Maris [5] explained the temperature dependence of the viscosity of $^4$He below 0.6 K in terms of the eigenvalues of the 3PP collision operator. Later, using a variational calculation, Benin [6] obtained similar results. Their fundamental idea is that the relaxation rate characterizing the viscosity is the eigenvalue of the 3PP collision operator with angular momentum quantum number $l = 2$. Although their results provide a good explanation for viscosity experimental data [7], in the development of their theories, over-simplified approximations were used for simplicity of the numerical calculation.

Maris, for example, used only the linear term in the expression for the anomalous phonon energy spectrum in the matrix element calculation, and for the procedure of transforming an integral eigenvalue problem into a matrix form he divided the range of the integral into a relatively small number of summing points (10–20). In Benin's theory, rather rough trial wave functions were used. The effects of these rough approximations in both theories can be shown in the behavior of the sequence of the lowest eigenvalues with increasing $l$ at a given temperature. Maris' theory [3,8] shows increasing behavior of the sequence with $l$, i.e., no saturation, and in Benin's variational theory this increasing behavior is more severe.

In general as $l$ increases, the angular distance $\theta_m$ between the maximum point and minimum point of the variation of the phonon distribution from an equilibrium value decrease inversely with $l$ ($\theta_m = \pi/l$). Roughly speaking, when $\theta_m/2$ becomes smaller than the average value of the scattering angle of 3PP at a given temperature, the lowest relaxation rates may be constant, which shows a saturated behavior. We provide our numerical results showing this saturated behavior in Sec. 3.

For the eigenvalues of the 3PP collision operator, Maris [8] obtained a discrete spectrum. According to our calculation, the spectrum of the eigenvalues with $l = 2$ is a continuous one having a finite positive minimum value. This continuous property of the eigenvalue spectrum seems to be in accordance with the theoretical work of Buot [9] about the relaxation rate spectrum of phonons. For the first-sound attenuation in $^4$He, a shoulder observed by Roach et al. [10] is explained to be the result of the restriction of 3PP, which means that the zero-temperature spectrum depends on pressure [11].

In present paper we obtain, using a similar method to Maris, the integral expression of the eigenvalue problem and convert it into a matrix form. From this collision matrix we calculate the eigenvalues and phonon viscosity for $^4$He below 0.6 K. From the diagonal elements of the collision matrix, we also give a natural explanation for the shoulder of the ultrasonic attenuation. In Sec. 2 the collision matrix for 3PP is constructed. The numerical analysis of the eigenvalues for the matrix is given in Sec. 3. In Sec. 4 we evaluate the viscosity and ultrasonic attenuation, and compare them with available experimental data. Conclusions are given in Sec. 5.

## 2. Collision matrix for three-phonon processes

In the long-wavelength limit, the interaction for 3PP is given by

$$V_3 = \int dr \left[ \frac{1}{2} m_4 v_s(r) \rho_4(r) v_s(r) + \frac{1}{6} \frac{\partial}{\partial n_4} \left( \frac{m_4 s^2}{n_4} \right) \rho_4(r)^3 \right], \tag{2.1}$$

where $m_4$ is the $^4$He mass, and $v_s(r)$ and $\rho_4(r)$ are the local superfluid velocity and local density variation of $^4$He from equilibrium density $n_4$, which are small quantities. These small variations can be expanded within a volume $V$ in terms of phonon annihilation and creation operators, $b_q$ and $b_q^+$, as

$$\rho_4(r) = \sum_q \left( \frac{q^2 n_4}{2 m_4 \omega_q V} \right)^{1/2} (b_q e^{iqr} + b_q^+ e^{-iqr}), \tag{2.2}$$

and

$$v_s(r) = \sum_q \left( \frac{\omega_q}{2 m_4 n_4 V} \right)^{1/2} \hat{q} (b_q e^{iqr} + b_q^+ e^{-iqr}), \tag{2.3}$$

where $\omega_q$ is the energy of a phonon with momentum $q$. We can then obtain the matrix element for 3PP by a straightforward calculation as

$$\langle q', q'' | V_3 | q \rangle = \left( \frac{T(q, q', q'')}{V} \right)^{1/2} \delta_{q'+q'', q}, \tag{2.4}$$

where

$$T(q, q', q'') =$$

$$= \left( \frac{1}{8 m_4 n_4} \right) \left[ \left( \frac{\omega_q \omega_{q''}}{\omega_{q'}} \right)^{1/2} q' \hat{q} \cdot \hat{q}'' + \left( \frac{\omega_q \omega_{q'}}{\omega_{q''}} \right)^{1/2} q'' \hat{q} \cdot \hat{q}' + \right.$$

$$\left. + \left( \frac{\omega_{q'} \omega_{q''}}{\omega_q} \right)^{1/2} q \hat{q}' \cdot \hat{q}'' + s^2 (2u - 1) \frac{q q' q''}{(\omega_q \omega_{q'} \omega_{q''})^{1/2}} \right]^2, \tag{2.5}$$

and $u$ is the Grüneisen constant defined by

$$u = \frac{n_4}{s} \frac{\partial s}{\partial n_4}, \tag{2.6}$$

with a value of 2.84 [12].

The collision integral due to the 3PP is given by

$$I_{3PP}(\mathbf{q}) = \frac{1}{2}\sum_{\mathbf{q}'\mathbf{q}''} 2\pi|\langle \mathbf{q}', \mathbf{q}''|V_3|\mathbf{q}\rangle|^2\, \delta(\varepsilon_f - \varepsilon_i)[n_{\mathbf{q}'}n_{\mathbf{q}''}(1+n_{\mathbf{q}}) -$$

$$- n_{\mathbf{q}}(1+n_{\mathbf{q}'})(1+n_{\mathbf{q}''})] + \sum_{\mathbf{q}',\mathbf{q}''} 2\pi|\langle \mathbf{q}'|V_3|\mathbf{q}\mathbf{q}''\rangle|^2\, \delta(\varepsilon_f - \varepsilon_i) \times [n_{\mathbf{q}'}(1+n_{\mathbf{q}''})(1+n_{\mathbf{q}}) - n_{\mathbf{q}'}n_{\mathbf{q}''}(1+n_{\mathbf{q}'})]\,, \tag{2.7}$$

where $\varepsilon_i$ and $\varepsilon_f$ are the phonon energy of initial and final state, respectively, and $n_{\mathbf{q}}$ is the distribution of phonons with momentum $\mathbf{q}$. In Eq. (2.7), the first term represents the process $\mathbf{q} \leftrightarrow \mathbf{q}' + \mathbf{q}''$ and the second term the process $\mathbf{q}' \leftrightarrow \mathbf{q} + \mathbf{q}''$.

If the phonons are in their equilibrium state, i.e., $n_{\mathbf{q}} = n^0_{\mathbf{q}}$, where $n^0_{\mathbf{q}}$ is the equilibrium phonon distribution, the collision integral vanishes by detailed balance. If we consider a small variation from the equilibrium as

$$n_{\mathbf{q}} = n^0_{\mathbf{q}} + \delta n_{\mathbf{q}}\,, \tag{2.8}$$

then the collision integral can be rewritten to first order in $\delta n_{\mathbf{q}}$ as

$$I_{3PP}(\mathbf{q}) = -\frac{1}{2(2\pi)^2}\int_{(1)} d\mathbf{q}'\, d\Omega_{\mathbf{q}'}\, q'^2 T(\mathbf{q},\mathbf{q}',\mathbf{q}'')\delta(\varepsilon_f - \varepsilon_i) \times [\delta n_{\mathbf{q}}(1 + n^0_{\mathbf{q}'} + n^0_{\mathbf{q}''}) - \delta n_{\mathbf{q}'}(n^0_{\mathbf{q}''} - n^0_{\mathbf{q}}) - \delta n_{\mathbf{q}''}(n^0_{\mathbf{q}'} - n^0_{\mathbf{q}})] -$$

$$- \frac{1}{(2\pi)^2}\int_{(2)} d\mathbf{q}'\, d\Omega_{\mathbf{q}'}\, q'^2 T(\mathbf{q}, \mathbf{q}', \mathbf{q}'')\delta(\varepsilon_f - \varepsilon_i) \times [\delta n_{\mathbf{q}}(n^0_{\mathbf{q}''} - n^0_{\mathbf{q}'}) - \delta n_{\mathbf{q}'}(1 + n^0_{\mathbf{q}} + n^0_{\mathbf{q}''}) + \delta n_{\mathbf{q}''}(n^0_{\mathbf{q}} - n^0_{\mathbf{q}'})]. \tag{2.9}$$

Due to momentum conservation, $\mathbf{q}'' = \mathbf{q} - \mathbf{q}'$ in the first integral and $\mathbf{q}'' = \mathbf{q}' - \mathbf{q}$ in the second integral, which are denoted by (1) and (2), respectively, in Eq. (2.9).

The variation of the distribution function from the equilibrium state can be expanded by spherical harmonics as

$$\delta n_{\mathbf{q}} = q\bar{n}^0_{\mathbf{q}} \sum_{l,m} \Phi_{lm}(q) Y_{lm}(\Omega_q)\,, \tag{2.10}$$

where for simplicity we define

$$\bar{n}^{\,0}_{\mathbf{q}} \equiv \frac{\partial n^0_{\mathbf{q}}}{\partial \omega_{\mathbf{q}}}\,. \tag{2.11}$$

$Y_{lm}(\Omega_q)$ is a spherical harmonic, and $\Omega_q$ is the solid angle of $\mathbf{q}$. Using the addition theorem, the spherical harmonics for $\mathbf{q}'$ and $\mathbf{q}''$ are transformed to those for $\mathbf{q}$ as follows:

$$Y_{lm}(\Omega_{q'}) \to P_l(\cos\theta) Y_{lm}(\Omega_q)\,, \tag{2.12}$$

$$Y_{lm}(\Omega_{q''}) \to P_l(\cos\theta') Y_{lm}(\Omega_q)\,, \tag{2.13}$$

where $P_l$ is the Legendre polynomial, and $\theta$ and $\theta'$ are the angles between momenta $(\mathbf{q}, \mathbf{q}')$ and momenta $(\mathbf{q}, \mathbf{q}'')$, respectively.

After performing the angular integration, we obtain the collision integral as

$$I_{3PP}(\mathbf{q}) = -q\bar{n}^{\,0}_{\mathbf{q}} \sum_{l,m} Y_{lm}(\Omega_q) \times$$

$$\times \left\{ \frac{1}{2(2\pi)} \int_{(1)} d\mathbf{q}' q'^2 \frac{T(\mathbf{q}, \mathbf{q}', \mathbf{q}'')}{B(\mathbf{q}, \mathbf{q}', \mathbf{q}'')} \left[ (1 + n^0_{\mathbf{q}'} + n^0_{\mathbf{q}''})\Phi_{lm}(q) - \frac{q'\bar{n}^{\,0}_{\mathbf{q}'}}{q\bar{n}^{\,0}_{\mathbf{q}}} (n^0_{\mathbf{q}''} - n^0_{\mathbf{q}}) P_l(\cos\theta)\Phi_{lm}(q') - \right.\right.$$

$$-\frac{q''\bar{n}^0_{q''}}{q\bar{n}^0_q}(n^0_{q'}-n^0_q)P_l(\cos\theta')\Phi_{lm}(q')\Big]+$$

$$+\frac{1}{2\pi}\int_{(2)}dq'\,q'^2\frac{T(\mathbf{q},\mathbf{q}',\mathbf{q}'')}{B(\mathbf{q},\mathbf{q}',\mathbf{q}'')}\Big[(n^0_{q''}-n^0_{q'})\Phi_{lm}(q)-\frac{q'\bar{n}^0_{q'}}{q\bar{n}^0_q}(1+n^0_q+n^0_{q''})P_l(\cos\theta)\Phi_{lm}(\mathbf{q}')+$$

$$+\frac{q''\bar{n}^0_{q''}}{q\bar{n}^0_q}(n^0_q-n^0_{q'})P_l(\cos\theta')\Phi_{lm}(q'')\Big]\Big\}\,, \tag{2.14}$$

where $B(\mathbf{q},\mathbf{q}',\mathbf{q}'')$, originating from the delta function representing energy conservation through 3PP, is defined by

$$B(\mathbf{q},\mathbf{q}',\mathbf{q}'')=\left|\frac{\partial(\varepsilon_f-\varepsilon_i)}{\partial\cos\theta}\right|\,. \tag{2.15}$$

If we represent the collision integral in terms of the relaxation time $\tau_l$, that is,

$$I_{3PP}(\mathbf{q})=-q\bar{n}^0_q\sum_{l,m}\frac{Y_{lm}(\Omega_q)\Phi_{lm}(q)}{\tau_l}\,, \tag{2.16}$$

we then obtain the eigenvalue equation for each $l$. Because the different values of $m$ do not change the form of the eigenvalue equation, we suppress the index $m$.

The eigenvalue equation for a given $l$ becomes

$$\frac{1}{2(2\pi)}\int_{(1)}d\,q'q'^2\frac{T(\mathbf{q},\mathbf{q}',\mathbf{q}'')}{B(\mathbf{q},\mathbf{q}',\mathbf{q}'')}\Big[(1+n^0_{q'}+n^0_{q''})\Phi_l(q)-\frac{q'\bar{n}^0_{q'}}{q\bar{n}^0_q}(n^0_{q''}-n^0_q)P_l(\cos\theta)\Phi_l(q')-$$

$$-\frac{q''\bar{n}^0_{q''}}{q\bar{n}^0_q}(n^0_{q'}-n^0_q)P_l(\cos\theta')\Phi_l(q'')\Big]+$$

$$+\frac{1}{2\pi}\int_{(2)}dq'\,q'^2\frac{T(\mathbf{q},\mathbf{q}',\mathbf{q}'')}{B(\mathbf{q},\mathbf{q}',\mathbf{q}'')}\Big[(n^0_{q''}-n^0_{q'})\Phi_l(q)-\frac{q'\bar{n}^0_{q'}}{q\bar{n}^0_q}(1+n^0_q+n^0_{q''})P_l(\cos\theta)\Phi_l(\mathbf{q}')+$$

$$+\frac{q''\bar{n}^0_{q''}}{q\bar{n}^0_q}(n^0_q-n^0_{q'})P_l(\cos\theta')\Phi_l(q'')\Big]=\lambda_l\,\Phi_l(q)\,, \tag{2.17}$$

where the eigenvalue $\lambda_l=\tau_l^{-1}$.

Since this integral eigenvalue equation can not be solved analytically, we use a numerical method. If we replace the integral on the left-hand side by a sum over a finite set of points, a matrix eigenvalue equation is obtained as

$$M_l\,\Phi_l=\lambda_l\,\Phi_l\,, \tag{2.18}$$

where $M_l$ denotes the collision matrix with a given $l$ symbolically. The diagonal elements of the matrix $M_l$ come from the terms containing $\Phi_l(q)$ in Eq. (2.17), while the terms containing $\Phi_l(q')$ or $\Phi_l(q'')$ give the off-diagonal elements. Then the number of eigenfunctions and eigenvalues is equal to the matrix size $j_m$, the number of points to be summed over.

## 3. Numerical analysis for the eigenvalues

### 3.1. Phonon energy spectrum

In order to perform numerical calculations we should choose an anomalous phonon energy spectrum to use. As we will see later, the wide-angle scattering rate depends sensitively on the phonon energy spectrum. Among the various spectra proposed by many authors, we take two forms, one suggested by Greywall [13] and another by

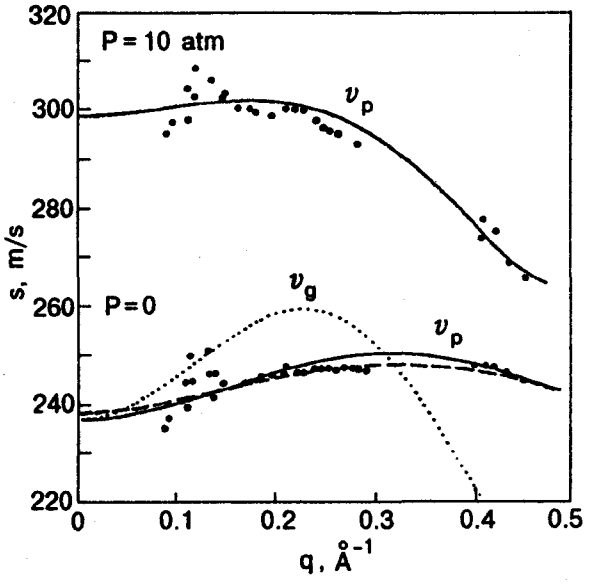


*Fig. 1.* Phase and group velocities at $P = 0$ and 10 atm. The solid lines are the phase velocities of Greywall's spectrum: the upper curve is for $P = 10$ atm and the lower curve for $P = 0$. The dashed line is Maris' phase velocity. The phase velocities of both spectra are consistent with neutron scattering experiments [14]. The dotted line represents Greywall's group velocity.

Maris [3]. The phonon energy spectrum suggested by Greywall is

$$\omega_q = sq\,(1 + \alpha_2 q^2 + \alpha_4 q^4 + \alpha_6 q^6)\,, \qquad (3.1)$$

where

$$s = 237.0 \text{ m/s for } P = 0 \text{ atm}\ ;$$

$$s = 298.9 \text{ m/s for } P = 10 \text{ atm}\ ;$$

$$\alpha_2 = 1.30 - 0.065P\ ;$$

$$\alpha_4 = -10.25\,\alpha_2 + 108.5\,(s_4/s - 1) - 28.44\,(s_5/s - 1);$$

$$\alpha_6 = 25.0\,\alpha_2 - 434.0\,(s_4/s - 1) + 177.8\,(s_5/s - 1)\ ;$$

$$s_4 = 247.0 + 2.86\,P\ ;$$

$$s_5 = 242.0 + 2.20\,P\ .$$

Here $s$ is the velocity of first sound and $P$ is the pressure. This spectrum has pressure dependence, so is available under arbitrary pressure. Another spectrum given by Maris is

$$\omega_q = sp\left(1 + \gamma p^2 \frac{1 - (p/p_A)^2}{1 + (p/p_B)^2}\right), \qquad (3.2)$$

where

$$s = 238.3 \text{ m/s}\ ;\ \gamma = 10 \times 10^{37} \text{ CGS units}\ ;$$

$$p_A/\hbar = 0.542 \text{ Å}^{-1}\ ;\ p_B/\hbar = 0.332 \text{ Å}^{-1}\ .$$

Let us test the properties of the above two spectra. Figure 1 shows the phase velocities of the two spectra and the group velocity of Greywall's spectrum at $P = 0$ atm. The phase velocity of Greywall's spectrum at $P = 10$ atm is also presented. It is shown that the phase velocities are consistent with neutron scattering experiments [14]. For the case of $P = 0$ atm, the maximum positions of the phase velocities, $v_p$, of both spectra are almost the same at about $q = 0.3$ Å$^{-1}$, while the maximum value of Greywall's is larger than that of Maris'. For $P = 10$ atm, the range of $v_p/s$ is reduced considerably compared to the case of $P = 0$, which is related closely to the cut-off momentum, $q_c$, above which 3PP do not occur.

For the above spectra, we obtain the allowed range for 3PP and the 3PP scattering angle, using conditions of energy and momentum conservation. The 3PP do not change the total momentum and total energy, so that the momentum and energy of the initial state equal those of the final state. For convenience, we denote $\mathbf{q} = \mathbf{q}' + \mathbf{q}''$ as the first process and $\mathbf{q}' = \mathbf{q} + \mathbf{q}''$ as the second process. For the case of the first process, for example, the energy and momentum conserve as

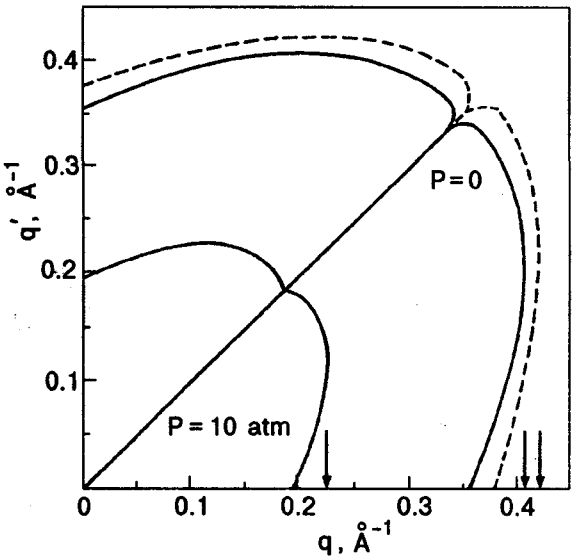


*Fig. 2.* The allowed range of 3PP for Greywall's spectrum (solid lines) at $P = 0$ and 10 atm and that of Maris' spectrum (dashed lines). The vertical arrows indicate the cut-off momenta. The lower part ($q > q'$) denotes the allowed range of the first process and the upper part ($q' > q$) that of the second process.

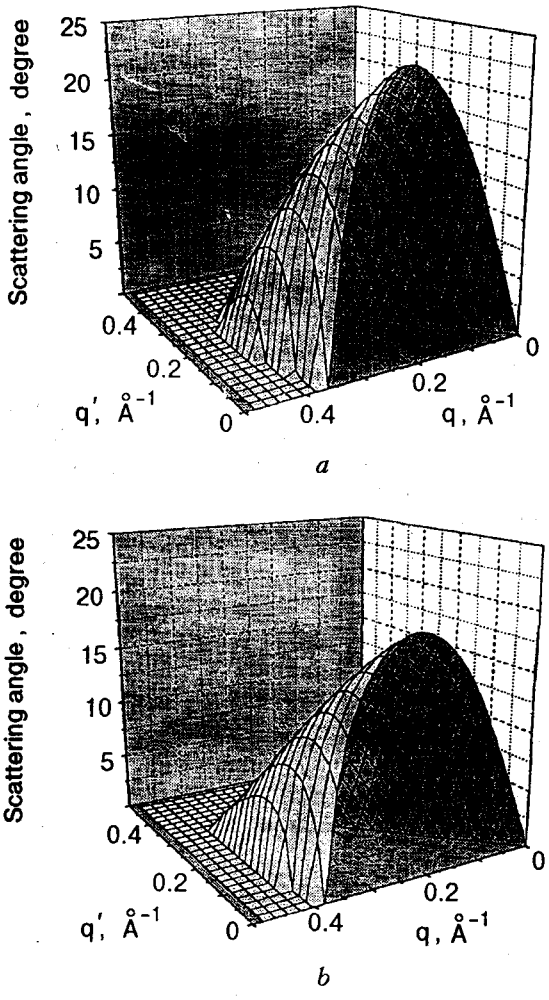


*Fig. 3.* 3PP scattering angle distribution of the first processes. Greywall's spectrum (*a*). Maris' spectrum (*b*).

$$\mathbf{q} = \mathbf{q}' + \mathbf{q}'' , \tag{3.3}$$

$$\omega_{\mathbf{q}} = \omega_{\mathbf{q}'} + \omega_{\mathbf{q}''} . \tag{3.4}$$

Using the above equations, we can determine the allowed range for 3PP in the $qq'$ plane, which is shown in Fig. 2. The lower part of the diagonal line in Fig. 2 is the region in which the first process is allowed, and the upper part corresponds to the second process. The allowed regions have symmetry about the diagonal line, i.e., under exchange of $q$ and $q'$ as expected. The changes of the range with pressure also are shown. As pressure increases, the allowed range for 3PP becomes smaller, which can be expected from the behavior of the phase velocity as a function of pressure in Fig. 1. We can see the cut-off momentum, $q_c$, for 3PP indicated by a vertical arrow in Fig. 2. We note that the allowed range for 3PP and cut-off momentum from Maris' spectrum are larger than those of Greywall's.

From the conditions of momentum and energy conservation, we also obtain the 3PP scattering angle distribution. The distribution of the 3PP scattering angle of the first process, i.e., the angle between $\mathbf{q}$ and $\mathbf{q}'$, is given in Fig. 3. The maximum scattering angle for Greywall's spectrum is 23.8°, which is larger than 19.6° for Maris' spectrum.

### *3.2. Numerical calculation of the eigenvalue*

The eigenvalues of the 3PP collision matrix with $l = 2$, $M_2$, are the relaxation rates characterizing the viscosity, because they are related to the phonon momentum transfer in the perpendicular direction. We note that the eigenvalues depend on the matrix size $j_m$. As we can see in Fig. 4, the eigenvalue spectrum becomes denser as $j_m$ increases. Such behavior of the eigenvalues indicates that the eigenvalue spectrum at infinite $j_m$ is continuous, unlike the result of Maris [8] in which a discrete eigenvalue spectrum is obtained. Only the lowest eigenvalue has physical importance because the corresponding eigenfunction, having no node, is appreciable in the range of momentum considered, while the eigenfunctions corresponding the eigenvalues just above the lowest one are negligible except for very small momentum. A similar argument for eigenvalues with $l = 1$ was given by Maris [8].

In Fig. 5, the temperature variation of the lowest eigenvalue $\lambda_2$ with $j_m$ are shown. We can see that $\lambda_2(T)$ converges with increasing $j_m$. This fact is

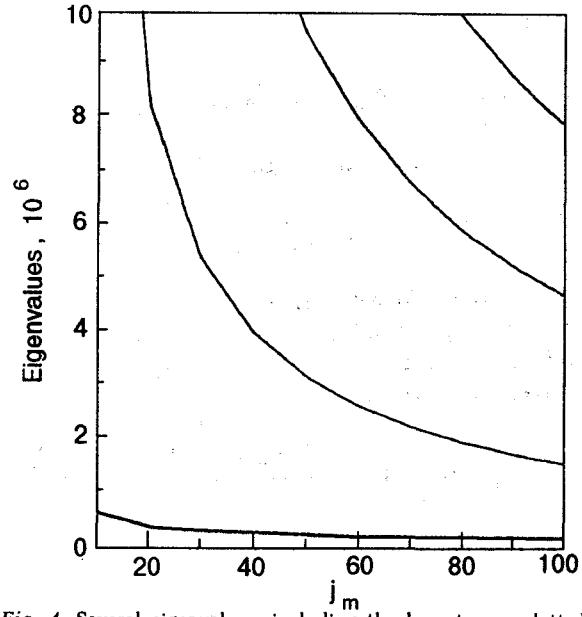


*Fig. 4.* Several eigenvalues, including the lowest one, plotted as matrix size $j_m$.

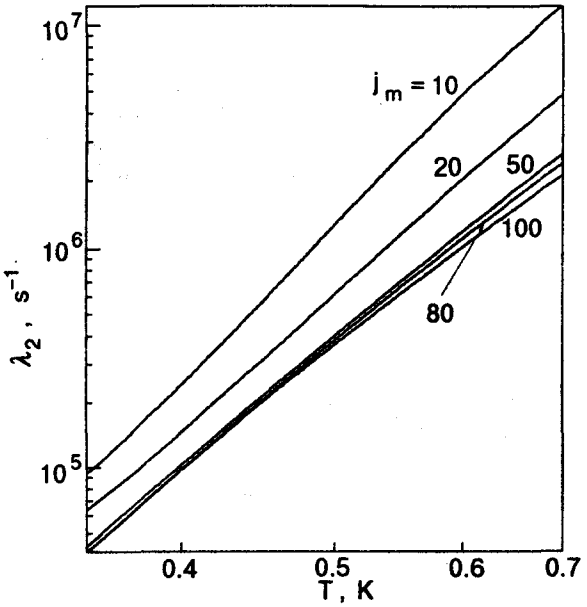


*Fig. 5.* Convergence of the lowest eigenvalues ($\lambda_2$) as a function of matrix size $j_m$.

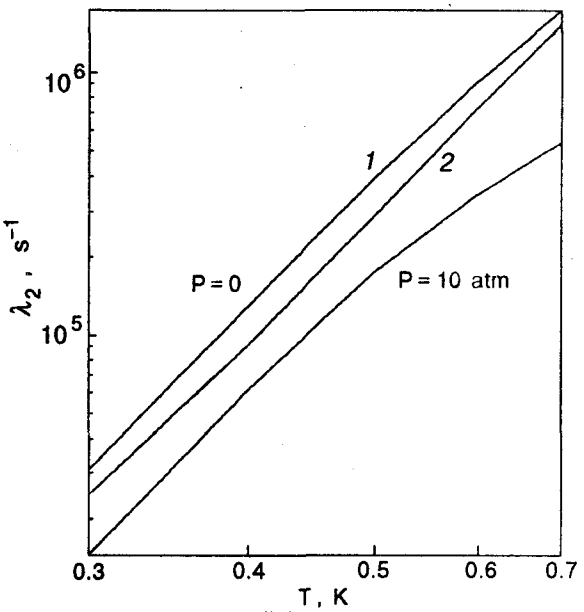


*Fig. 7.* Lowest eigenvalues ($\lambda_2$) as a function of $T$. Greywall's spectrum (*1*), Maris' spectrum (*2*). The case of $P = 10$ atm from Greywall's spectrum is also shown.

different from Maris' argument that, for $j_m = 15$, $\lambda_2(T)$ is independent of the details of the mesh to better than 1%.

We also obtain the lowest eigenvalues for several $l$ as shown in Fig. 6. A saturated behavior appears when we take $j_m = 100$, which means that the phonons relax sufficiently in one collision time. At higher temperatures this saturated behavior may begin to appear at smaller $l$, since the typical 3PP scattering angle increases due to the higher average value of momentum (Fig. 3). Figure 6 shows this

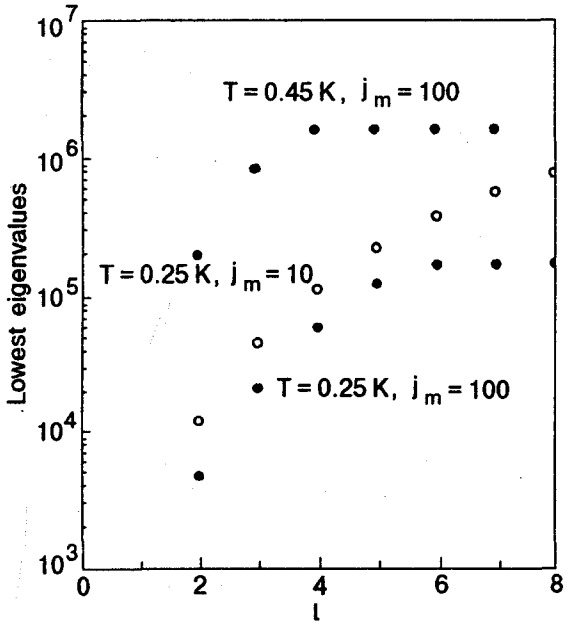


*Fig. 6.* Lowest eigenvalues versus $l$.

behavior correctly. On the other hand, the results obtained by Maris [8] and Benin [6] have no saturated behavior. Their results are very similar to the case of $j_m = 10$ in our calculation. But $j_m = 10$ is too small to reveal the properties of the anomalous spectrum correctly. Therefore, we guess that their results with no saturation are due to the rough approximations in their numerical calculations.

Using both spectra presented before, we calculate the lowest eigenvalues $\lambda_2$ as a function of temperature by taking $j_m = 300$ and the upper bound of the integral of Eq. (2.17), $q_m = 0.45$ Å$^{-1}$, i.e., $\Delta q = 0.0015$ Å$^{-1}$. This value of $q_m$ is enough to cover the effective range of the integral, because the cut-off momentum $q_c$ at $P = 0$ is about 0.4 Å$^{-1}$ as shown in Fig. 2. The results are shown in Fig. 7. When Greywall's spectrum is used, the values of $\lambda_2(T)$ are larger than those of Maris. This can be understood from the fact that the maximum value of the 3PP scattering angle distribution for Greywall's spectrum is greater than that of Maris'. Using Greywall's spectrum with $P = 10$ atm, we also obtain a smaller $\lambda_2(T)$ than for the case of $P = 0$, which is a trivial result because the cut-off momentum and 3PP scattering angle become smaller as pressure increases.

## 4. Viscosity and ultrasonic attenuation

### *4.1. Viscosity*

The viscosity is written in terms of the phonon mean free path characterizing the viscosity [3] as

$$\eta = \frac{1}{5} \rho_{ph} \langle v_g \rangle \Lambda , \qquad (4.1)$$

where $\rho_{ph}$ is the phonon mass density defined by

$$\rho_{ph} = -\sum_{q} \frac{q^2}{3} \frac{\partial n_q^0}{\partial \omega_q} , \qquad (4.2)$$

and $\langle v_g \rangle$ is the average of the phonon group velocity

$$\langle v_g \rangle \equiv -\frac{1}{\rho_{ph}} \sum_{q} \frac{q^2}{3} \frac{\partial n_q^0}{\partial \omega_q} \frac{d\omega_q}{dq} . \qquad (4.3)$$

The mean free path for 3PP is related to the eigenvalues of the collision matrix as

$$\Lambda = \frac{\langle v_g \rangle}{\lambda_2} . \qquad (4.4)$$

The results for $\Lambda$ are depicted in Fig. 8. The dashed line denotes the mean free path due to 4PP calculated by Landau and Khalatnikov [15], which has a $T^{-9}$ dependence. At $P = 0$, the mean free path from Maris' spectrum, drawn by the dotted line, shows good agreement with the experiment performed on thermal conductivity by Greywall [13]. The mean free path from Greywall's spectrum appears to be lower than the experimental data. It can be well deduced, at least qualitatively, from the higher maximum value of the 3PP scattering angle in Fig. 3 and the larger phase velocity in Fig. 1.

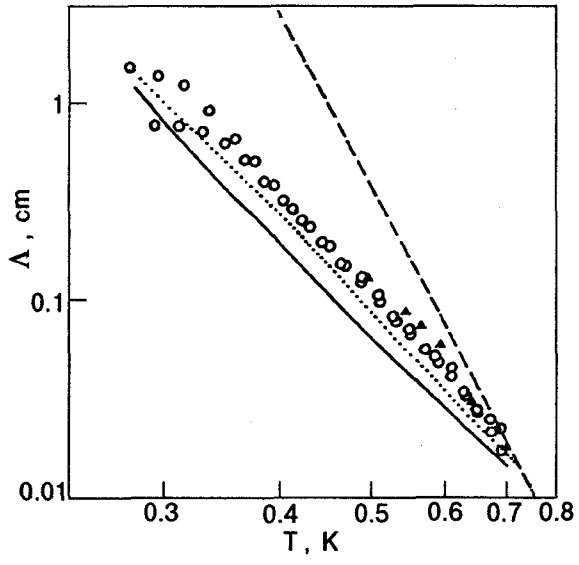


*Fig. 8.* Phonon mean free path resulting from 3PP. The solid line represents the result using Greywall's spectrum, and the dotted line that using Maris' spectrum. The open circles and the triangular marks indicate the experimental data on thermal conductivity by Greywall [13] and Whitworth [7], respectively. The dashed line shows the theory of Landau and Khalatnikov based on 4PP [15].

### *4.2. Ultrasonic attenuation*

At low pressures, the temperature dependence of the high-frequency ultrasonic attenuation ($\alpha$) is approximately described by a $T^4$ law as under vapor pressure, whereas at higher pressures ( $\geq$ 10 atm) the $\alpha(T)$ curve is significantly changed, and a shoulder occurs [10]. Roach et al. [10] suggested that the shoulder might indicate the existence of a new relaxation mechanism. However, Jäckle and Kehr [11] showed that the formation of the shoulder in $\alpha(T)$ is explained by assuming that the 3PP is allowed only for very long-wavelength phonons («partially allowed 3PP») due to deformation of the phonon spectrum under pressure.

Now we show the appearance of the shoulder using the collision matrix introduced in the previous section. The ultrasonic sound means very long-wavelength phonons, which are injected from outside of the system. So, we can suppose that thermal phonons are in equilibrium, and only very long-wavelength phonons have variation from equilibrium due to the injected sound phonons.

Let the momentum of sound phonons be $q$. For thermal phonons with momenta $q'$ and $q''$ in the equilibrium state,

$$\Phi_l(q') = 0 , \qquad (4.5)$$

$$\Phi_l(q'') = 0 \qquad (4.6)$$

in the collision integral of Eq. (2.17). Then only the terms containing $\Phi_l(q)$ remain, which means that only the diagonal elements of the collision matrix are nonzero. Then the $l$-dependence of the collision matrix equation disappears. The absorption rate, $\Gamma_a(q)$, of sound phonon by thermal phonon, therefore, becomes the diagonal part of the collision matrix.

The attenuation of sound is related to the absorption rate as

$$\alpha = \frac{\Gamma_a(q)}{2s} . \qquad (4.7)$$

Therefore, if we know the phonon energy spectrum under pressure, the attenuation of first sound can be obtained. Figure 9 shows the results for the attenuation of ultrasonic sound. For temperatures below 0.6 K the results show good agreement with experimental data. The parameters of the phonon energy spectrum used in this calculation are listed in Table. The maximum scattering angle $\theta_m$ and cut-off mo-

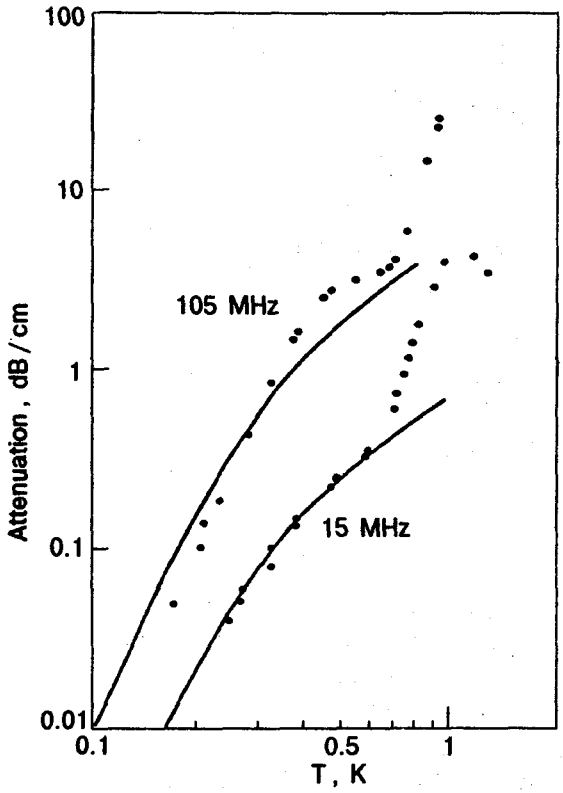


*Fig. 9.* Ultrasonic attenuation for different frequencies under pressure 16.4 atm. The solid points are the experimental data of Roach et al. [10].

mentum $q_c$ calculated by these parameters are also listed in Table. We find that for the case of attenuation of sound, the process $\mathbf{q} + \mathbf{q}'' \rightarrow \mathbf{q}'$ is dominant. This means that the sound phonons are absorbed by thermal phonons. The scattering in this case is almost linear since the maximum scattering angle is $\theta_m = 0.83°$, and only very long-wavelength phonons, $q < 0.0625$ Å$^{-1}$ , take part in the scattering. The cut-off momentum obtained here shows remarkable agreement with the result of Jäckle and Kehr (within 1%). The rapidly increasing behavior at high temperature, $T > 0.6$ K, can be explained by considering the existence of rotons [11], and so for this temperature range the contribution of rotons is essential.

Table

Phonon spectrum parameters used in the calculation of the sound attenuation at $P = 16.4$ atm

| $s$, m/s | $\alpha_2$, Å$^2$ | $\alpha_4$, Å$^4$ | $\alpha_6$, Å$^6$ | $\theta_m$, degree | $sq_c/k_B$, K |
|---|---|---|---|---|---|
| 332.4 | 0.0454 | −8.3 | 22.35 | 0.83 | 1.59 |

## 5. Conclusions

We obtain the wide-angle scattering rates and the absorption rates of phonons in $^4$He below 0.6 K by solving the eigenvalue equation for the 3PP collision matrix. The sequence of the lowest eigenvalues of the collision matrix along $l$ shows a saturated behavior, which is different from the results given by Maris and Benin. With Maris' and Greywall's phonon spectra, we calculate the viscosity mean free paths and compare them with experimental data, where the Maris' spectrum is seem to be in better agreement. For the result of ultrasonic attenuation, the phonon spectrum parameters at $P = 16.4$ atm are obtained from a fit, and the cut-off momentum calculated from the parameters is in excellent agreement with Ref. 11.

Since the 3PP are also an important phonon-phonon mechanism in dilute $^3$He–$^4$He mixtures at low temperatures, it is possible to apply this theory to such mixtures. This study is in progress.

## Acknowledgements

This work was supported by the Research Institute of Basic Science in Korea University and Non-directed Research Fund, Korea Research Foundation, 1995.

1. H. J. Maris and W. E. Massey, *Phys. Rev. Lett.* **25**, 220 (1970).
2. H. J. Maris, *Phys. Rev. Lett.* **28**, 277 (1972).
3. H. J. Maris, *Phys. Rev. Lett.* **30**, 312 (1973).
4. C. I. Um, C. W. Jun, and T. F. George, *Phys. Rev.* **B46**, 5746 (1992).
5. H. J. Maris, *Phys. Rev.* **A8**, 1980 (1973).
6. D. Benin, *Phys. Rev.* **B11**, 145 (1975).
7. R. W. Whitworth, *Proc. R. Soc. London* **A246**, 390 (1958).
8. H. J. Maris, *Phys. Rev.* **A9**, 1412 (1974).
9. F. A. Buot, *J. Phys.* **C5**, 5 (1972).
10. P. R. Roach, J. B. Ketterson, and M. Kuchnir, *Phys. Rev. Lett.* **25**, 1002 (1970).
11. J. Jäckle and K. W. Kehr, *Phys. Rev. Lett.* **27**, 654 (1971).
12. B. M. Abraham, Y. Eckstein, J. B. Ketterson, M. Kuchnir, and P. R. Roach, *Phys. Rev.* **A1**, 250 (1970); *ibid* **A2**, 550 (1970).
13. D. S. Greywall, *Phys. Rev.* **B23**, 2152 (1981).
14. W. G. Stirling, J. R. D. Copley, and P. A. Hilton, *Proc. Int. Symp. on Neutron Inelastic Scattering*, I.A.E.A., Vienna (1977).
15. L. D. Landau and I. M. Khalatnikov, *JETP* **19**, 637, (1949), *ibid* **19**, 709 (1949).